Tree Physiology 31, 178–195
doi:10.1093/treephys/tpr005

Research paper

Seasonal fluctuations and temperature dependence in photosynthetic parameters and stomatal conductance at the leaf scale of *Populus euphratica* Oliv.

Gao-Feng Zhu[1,3], Xin Li[2], Yong-Hong Su,[2,4,5], Ling Lu[2] and Chun-Lin Huang[2]

[1]Key Laboratory of Western China's Environmental Systems (Ministry of Education), Lanzhou University, Lanzhou 730000, China; [2]Cold and Arid Regions Environmental and Engineering Research Institute, Chinese Academy of Sciences, Lanzhou 730000, China; [3]The School of Mathematics, Physics and Software Engineering, Lanzhou Jiaotong University, Lanzhou 730030, China; [4]Present address: Cold and Arid Regions Environmental and Engineering Research Institute, Chinese Academy of Sciences, Donggang West Road 320, Lanzhou City, Gansu Province, China; [5]Corresponding author (syh@lzb.ac.cn)

Received September 21, 2010; accepted January 26, 2011; published online March 15, 2011; handling Editor Ülo Niinemets

A combined model to simulate CO_2 and H_2O gas exchange at the leaf scale was parameterized using data obtained from in situ leaf-scale observations of diurnal and seasonal changes in CO_2 and H_2O gas exchange. The Farquhar et al.-type model of photosynthesis was parameterized by using the Bayesian approach and the Ball et al.-type stomatal conductance model was optimized using the linear least-squares procedure. The results show that the seasonal physiological changes in photosynthetic parameters (e.g., V_{cmax25}, J_{max25}, R_{d25} and g_{m25}) in the biochemical model of photosynthesis and m in the stomatal conductance model should be counted in estimating long-term CO_2 and H_2O gas exchange. Overall, the coupled model successfully reproduced the observed response in net assimilation and transpiration rates.

Keywords: Bayesian statistics, Farquhar et al. model, maximum electron transport rate (J_{max}), maximum rate of Rubisco carboxylation (V_{cmax}), photosynthesis, stomatal conductance, transpiration, *Populus euphratica* Oliv.

Introduction

Predictions of forest carbon and water balances are necessary in order to answer many scientific questions, such as the effects of management on carbon sequestration, groundwater recharge and climate (e.g., Walker et al. 2002, Lasch et al. 2005, Silva et al. 2006, Vano et al. 2006, White et al. 2006) and the impacts of global change on forest production and water use (e.g., Hatton et al. 1992, Gordon and Famiglietti 2004, Morales et al. 2005, Gedney et al. 2006). Therefore, simultaneous estimations of CO_2 and H_2O gas-exchange coupling of the Farquhar et al. (1980)-type biochemical model of photosynthesis (hereafter, the FvCB model) and the Ball et al. (1987)-type stomatal conductance model (BWB model) have been reported in many articles (e.g., Collatz et al. 1991, Harley et al. 1992, Leuning et al. 1995, Kosugi et al. 2003). Although this coupled-model approach has become an important tool for understanding CO_2 and H_2O gas exchange at both the leaf and canopy scales, the parameterization of these models is still insufficient (Kosugi et al. 2003). Of the parameters concerning the net CO_2 assimilation rate, we have a good understanding of how photosynthesis model parameters [i.e., maximum carboxylation velocity (V_{cmax}), maximum rate of electron transport (J_{max}) and dark respiration (R_d)] vary with genus and species, plant functional type and leaf nitrogen content (Wullschleger 1993). With respect to the stomatal coefficient (m) of the BWB model, the majority of published studies were based on short-term measurements for well-watered C_3 species. Little is known, however, about the seasonal and temperature responses of the gas-exchange parameters of various species during the course as leaves expand, age, experience stress, acclimate and senesce (Wilson et al. 2000, Medlyn et al. 2002, Nogues and Alegre 2002, Xu and Baldocchi 2003).

This state of affairs arises because the FvCB model is not easy to parameterize due to its non-linearity and discontinuous differentiability (Medlyn et al. 2002, Su et al. 2009), and the methods used in estimating parameters of interest have not received much attention (Dubois et al. 2007). Traditionally, the photosynthetic parameters were obtained by fitting the FvCB model to leaf-level photosynthetic gas-exchange measurements (e.g., photosynthetic response to changes in intercellular CO_2 concentration; A–C_i curves). These analyses have been invaluable for elucidating and quantifying in vivo the fundamental biochemical processes underlying the photosynthetic responses of plants to various environmental conditions (Von Caemmerer 2000). However, the parameters estimated from the analysis of an A–C_i curve only correspond to measured temperature (Sharkey et al. 2007). Thus, to determine the temperature dependence of the photosynthetic parameters, a family of A–C_i curves must be investigated at various leaf temperatures, which is equipment intensive and laborious (Medlyn et al. 2002, Kosugi et al. 2003). To date, there is still a dearth of information regarding the temperature responses of the photosynthetic parameters (Leuning 1997, Medlyn et al. 2002). Also, this procedure of parameterization implicitly assumes that the kinetic properties of Rubisco (e.g., K_c, K_o and Γ^*) are relatively conserved in C_3 plants (Harley et al. 1986). Recent research has shown that these properties also change across diverse species and environmental conditions (Tcherkez et al. 2006). Therefore, the accuracy of fitting the FvCB model needs correct representation of the kinetic properties of Rubisco (Sharkey et al. 2007). Finally, it is important to determine the magnitude and seasonal fluctuations in leaf gas-exchange parameters for long-term gas-exchange modeling.

Recently, the Bayesian approach has been introduced to incorporate prior probabilistic density functions (PDFs) with measurements to generate posterior PDFs for parameters of ecosystem models (Braswell et al. 2005, Knorr and Kattge 2005). This not only allows the simultaneous determination of all parameters, it also allows consideration of prior knowledge for all parameters and accommodation of unknown influences (Clark 2005, Janes and Gelfand 2006, Knorr and Kattge 2005). Abundant evidence has shown that the Bayesian approach is advantageous for modeling plant physiological responses and photosynthesis (Cable et al. 2008, 2009, Ogle and Barber 2008, Ogle et al. 2009, Patrick et al. 2009*a*, 2009*b*). Also, advances in portable equipment enable us to get in situ leaf-scale observations on diurnal and seasonal changes of gas exchange and we have been accumulating data (Kosugi et al. 2003). Our research is motivated by a desire to implement a Bayesian framework that couples the FvCB model with the in situ diurnal and seasonal gas exchanges, allowing simultaneous estimates of the kinetic, photosynthetic and temperature dependence parameters. It is expected that the Bayesian approach integrating in situ measurements that cover diurnal and seasonal changes will be able to assess the 'actual' response of leaves in field conditions (Kosugi et al. 2003), and this procedure could perform as a complement to the A–C_i curve fitting method for investigating the photosynthetic characteristics of species of interest.

Thus, the purpose of our study was to determine values of parameters for the FvCB model and stomatal coefficient (m) for the BWB model of the investigated desert plant species (*Populus euphratica* Oliv.) leaves and to examine the seasonal and temperature response of these parameters. The specific objectives addressed were: (i) to illustrate and evaluate the potential of the Bayesian approach in the solution of the parameterization problem of the FvCB model using in situ leaf-scale observations on diurnal and seasonal changes of gas exchange, and briefly provide some details of implementation of the Bayesian calibration procedure; (2) to investigate seasonal fluctuations of the parameters associated with the coupled model such as the kinetic constant, photosynthetic parameter, temperature dependence parameters and stomatal coefficient; and (3) to determine whether it is possible to evaluate the CO_2 and H_2O gas exchange of temperate deciduous broad-leaved desert plants in all seasons with a single set of leaf gas-exchange parameters. Achieving these objectives should provide increased accuracy of leaf, canopy and global vegetation models and improve our understanding of the mechanism underlying the seasonal variation of photosynthesis and transpiration processes.

Materials and methods

Study sites, plants and field observations

The study was carried out on a single mature *P. euphratica* Oliv. tree growing in the poplar reserve (42°21′N, 101°15′E; elevation 920.5 m a.s.l.; 13.33 km^2) at Qidaoqiao, southeast of Ejina City, Inner Mongolia, China. This region is one of the most arid in China, evaporation exceeds 3500 mm year^{-1}, and mean annual rainfall (84% of which occurs during the growing season) is 36.6 mm year^{-1}. The annual mean air temperature is about 8.28 °C. The annual mean relative humidity is 42–35% and the moisture index is <0.009–0.012%. *Populus euphratica* Oliv. is the dominant native woody species in the reserve, whose average age is 25 years, and growth status is good. The stem density is 500 plants ha^{-1}. The mean tree height is 10 m and the mean diameter at breast height (DBH) is 0.12 m. Leaf flush of *P. euphratica* Oliv. starts in late March (March 24). In middle May (May 12), leaves begin to unfold rapidly and reach full expansion about 2 weeks later (May 26). Leaf senescence (yellowing of leaves) begins in middle September (September 18) and leaves are shed by late October or early November. The region's soil type is a poplar-forest soil varying from clay loam to sand. Organic matter content at the study site was 0.724% in the 0–0.3 m soil layer and 0.127% in the

0.3–2.0 m soil layer. The depth to the groundwater table ranged from 1.5 to 3.5 m.

Measurements were conducted during the 2008 growing season (May–September) on the following dates: May 29, June 20, July 22, August 18 and September 4. A mature tree was selected for periodic measurements of the study based on the principle of non-shading of the crown canopy. The DBH, height and crown spread of the selected tree were 0.21 m, 10.2 m and 230 cm × 230 cm, respectively. The canopy was accessed using hydraulic personnel lifts (Model UL 48; UpRight, Inc., Selma, CA, USA) positioned near the selected tree. The aerial work platforms extended up to 15.5 m, providing access to multiple crown positions.

Leaf gas exchange was measured using a portable photosynthesis system (LI-6400; Li-Cor, Lincoln, NE, USA). The system was operated in open flow mode with a 6-cm^2 leaf chamber and an integrated CO_2 supply system. For each of the 5 months, diurnal net assimilation (A) and stomatal conductance (g_s) rates, together with micro-climate variables such as photosynthetic quantum flux density (Q), air and leaf temperature (T_a and T_L), relative humidity (h_s), and intercellular and ambient CO_2 concentration (C_i and C_a), of three to four sunlit leaves were measured in situ every half-hour from early morning to sunset. Immediately prior to the start of a measurement, the leaf chamber was modified with an attached Peltier cooling system to maintain chamber temperature near ambient atmospheric temperature. Humidity in the gas-exchange cuvette was not controlled except to avoid condensation inside the gas-exchange system during early morning and evening measurements. The sunlit leaf was randomly selected with the criteria that it was located at the outer portions of a branch on the upper canopy, was intact and undamaged, and was similar to surrounding leaves. After the measurement was completed, the measured leaves were harvested to determine area, dry weight and nitrogen concentration. Leaf area was measured with a leaf area meter (LI-3100; Li-Cor). After that, leaves were dried for 48 h at 65 °C, dry weights were obtained, and then samples were ground and re-dried at 75 °C for several hours for determination of total nitrogen concentration with a CNS analyzer (Carlo Erba/Thermo Electron, Milan, Italy). Nitrogen concentrations were calibrated and checked against known standards.

Environmental conditions were measured at a meteorological observation tower. Air temperature and relative humidity above the canopy were measured with a Vaisala-type hygrothermometer (HMP-35C; Campbell Scientific), downward solar radiation was measured with a four-component radiometer (MR-40; Eiko, Japan), and rainfall data were from the Ejina Meteorological Bureau located ~3 km from the plantation. Volumetric soil water content was measured with a water content reflectometer (CS615; Campbell Scientific) buried at depths of 10, 20, 30, 40, 60, 80, 100 and 120 cm.

Model description

The combined model used for the estimation consists of a Farquhar et al. (1980)-type biochemical sub-model of photosynthesis for C_3 plants (FvCB model) and a Ball et al. (1987)-type stomatal conductance sub-model (BWB model). Following Ethier and Livingston (2004) and Niinemets et al. (2004, 2009*a*), the net CO_2 assimilation rate in the FvCB sub-model is described by

$$A = \min\{A_c, A_j\} \tag{1}$$

$$A_c = \frac{-b + \sqrt{b^2 - 4ac}}{2a} \tag{2}$$

$$a = -1 / g_m$$

$$b = \frac{V_{cmax} - R_d}{g_m} + C_i + K_c\left(1 + \frac{O}{K_o}\right)$$

$$c = R_d\left(C_i + K_c\left(1 + \frac{O}{K_o}\right)\right) - V_{cmax}(C_i - \Gamma^*)$$

$$A_j = \frac{-b + \sqrt{b^2 - 4ac}}{2a} \tag{3}$$

$$a = -1 / g_m$$

$$b = \frac{(J / 4 - R_d)}{g_m} + C_i + 2\Gamma^*$$

$$c = R_d(C_i + 2\Gamma^*) - J / 4(C_i - \Gamma^*)$$

$$\theta J^2 - (\alpha Q + J_{max})J + \alpha Q J_{max} = 0 \tag{4}$$

where A is the net CO_2 assimilation rate (μmol m^{-2} s^{-1}); min{} denotes 'the minimum of'; A_c and A_j are the RuBP-saturated and RuBP-limited net CO_2 assimilation rate, respectively (μmolm^{-2}s^{-1}); g_m is mesophyll conductance (μmolm^{-2}s^{-1}Pa^{-1}); C_i and O are partial pressure of CO_2 and O_2 at the sites of carboxylation and oxygenation, respectively (Pa or kPa); Γ^* is the CO_2 compensation point in the absence of mitochondrial respiration (Pa), and K_c and K_o are Michaelis–Menten constants for RuBP carboxylation and oxygen, respectively (Pa or kPa); V_{cmax} is the maximal CO_2 carboxylation rate (μmol m^{-2} s^{-1}); J is the potential rate (μmol m^{-2} s^{-1}) of electron transport, which is dependent upon incident light irradiance [i.e., photosynthetic quantum flux density (Q, μmol m^{-2} s^{-1})]; J_{max} is the light-saturated rate of electron transport (μmol m^{-2} s^{-1}); R_d is the mitochondrial respiration in light (μmol m^{-2} s^{-1}); θ is the curvature of the light response curve; and α is the quantum yield of electron transport. Because θ and α do not vary much among C_3 species (Niinemets et al. 1998, Medlyn et al. 2002, Kosugi et al. 2003), a general set of constant values was used in our study. The value of α was fixed at 0.3 mol electrons mol^{-1} photon, based on an average C_3 photosynthetic quantum yield of 0.093 and a leaf absorptance of 0.8 (Long et al. 1993). The value of θ was taken to be 0.90. Triose phosphate use (TPU) limitation was not considered here because this process is expected to rarely limit photosynthesis and is not commonly included in models to estimate photosynthesis parameters (Niinemets and Tenhunen 1997, Wohlfahrt et al. 1999, Medlyn et al. 2002, Kosugi et al. 2003, Gao et al. 2004, Dubois et al. 2007, Niinemets et al. 2009*a*, Patrick et al. 2009*a*).

The Arrhenius function (Von Caemmerer 2000, Leuning 2002, Medlyn et al. 2002, Kattge and Knorr 2007) is used for the temperature dependence of parameters K_c, K_o, Γ^* and R_d:

$$Y = Y_{25} \exp\left[\left(1 - \frac{T_{ref}}{T_L}\right)\frac{E_Y}{RT_{ref}}\right] \tag{5}$$

where Y_{25} is the parameter at 25 °C, E_Y is the activation energy of Y, T_L is the leaf temperature (in K) measured by Li-6400, T_{ref} is the reference temperature (298 K) and R is the universal gas constant (8.314 J mol^{-1} K^{-1}). Alternatively, a peaked function (Von Caemmerer 2000, Leuning 2002, Medlyn et al. 2002, Kattge and Knorr 2007) was used to determine the temperature dependence of g_m, V_{cmax} and J_{max}:

$$Y = Y_{25} \exp\left[\frac{E_Y(T_L - T_{ref})}{RT_{ref}T_L}\right]\frac{1 + \exp((T_{ref}\Delta S_Y - H_Y)/T_{ref}R)}{1 + \exp((T_L\Delta S_Y - H_Y)/T_L R)} \tag{6}$$

where H_Y is the deactivation energy, which describes the rate of decrease above the optimum temperature, and ΔS_Y is an entropy factor. The optimum temperatures (T_{opt}, also in K) of g_m, V_{cmax} and J_{max} are related by (Medlyn et al. 2002)

$$T_{opt} = \frac{H_Y}{\Delta S_Y - R\ln[E_Y/(H_Y - E_Y)]} \tag{7}$$

In sub-model BWB, stomatal conductance is estimated from the net assimilation rate (A), relative humidity (h_s) and CO_2 concentration at the leaf surface (C_s) using

$$g_{sw} = m\frac{Ah_s}{C_s} + g_{swmin} \tag{8}$$

where g_{sw} is the stomatal conductance of H_2O (mol m^{-2} s^{-1}), m is the slope of the relationship between the stomatal index (Ah_s/C_s) and the stomatal conductance, and g_{swmin} is the minimum stomatal conductance.

Under steady-state conditions, C_i can be estimated using the stomatal conductance of CO_2 (g_{sc}):

$$C_i = C_s - \frac{A}{g_{sc}} \tag{9}$$

where g_{sc} is the stomatal conductance to CO_2 such that $g_{sc} = (g_{sw}/1.6)$. The transpiration rate, E, can be calculated as

$$E = g_{sw}\,\mathrm{VPD} \tag{10}$$

where VPD is the water vapor pressure deficit between intercellular space and the air layer just above the leaf surface.

Coupling the models

The FvCB model uses C_i, among others leaf temperature (T_L) and photosynthetic quantum flux density (Q), as driving variables. The BWB model requires the net photosynthesis (A) as an input, while C_i results from the interaction of A and g_{sw}. Therefore, the two sub-models are interdependent. A nested iterative procedure was used to solve this relationship numerically (Figure 1). In finding the solution, the value of C_i was assumed to be equal to 0.7C_s, and was substituted into the biochemical photosynthesis model [Eq. (1)] to obtain an estimate of A. Then stomatal conductance (g_{sw}) was calculated from the stomatal model [Eq. (8)], and a new C_i ($C_{i\text{-new}}$) was estimated using the resulting A and g_{sc} [Eq. (9)]. This process was solved iteratively using the Newton–Raphson method

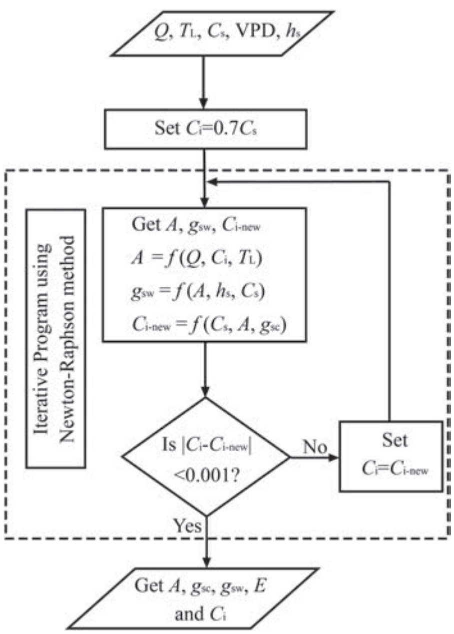

Figure 1. Schematic diagram of the coupled models flow.

until the change in C_i was less than a certain small value of allowance. It should be noted that the parameters of the FvCB and BWB sub-models must first be calibrated individually (discussed below).

Parameterization procedure

Data obtained under naturally varying conditions of photosynthetic quantum flux density (Q), leaf temperature and h_s, not curves obtained under CO_2, light, temperature or humidity-controlled conditions, were used to parameterize the two sub-models. The FvCB sub-model parameters were calibrated using the Bayesian method. The procedure begins by quantifying the uncertainty about parameter values in the form of so-called prior probability distributions. Then measured data on the output variables (e.g., net CO_2 assimilation rate) were used to yield an updated posterior distribution of the parameters. Herein, the Metropolis–Hasting algorithm (Metropolis et al. 1953, Hasting 1970), a version of the Markov chain Monte Carlo (MCMC) technique (Gelfand and Smith 1990, Gelman and Rubin 1992), was adopted to generate a representative sample of parameter vectors from the posterior distribution. This is achieved by multiplying the prior with its corresponding data likelihood function, which usually assumes that the model error (e.g., the difference between the simulated and observed outputs) is independent and normally distributed with mean zero (Van Oijen et al. 2005, Svensson et al. 2008). In practice, calculations were carried out using logarithms to avoid rounding errors because the data likelihood values easily become very small as the number of data points increases. Thus, the logarithm of the data likelihood function is set up as

$$\log L = \sum_{i=1}^{n}\left[-0.5\left(\frac{y_i - f(x_i;\,\lambda)}{\delta_i}\right)2 - 0.5\log(2\pi) - \log(\delta_i)\right] \quad (11)$$

where n is the number of data points, y_i is the measured CO_2 assimilation rate for observation i ($i = 1, 2, \ldots, n$), x_i is the vector of model input data, $f(x_i;\,\lambda)$ is the model simulation of y_i with the parameter vector λ and δ_i is the standard deviation of the model error.

The prior distributions of the calibration parameters are chosen as normal distribution centered on values reported in the literature (Table 1) and non-correlated. The first step of MCMC is to run an initial simulation with parameter values from an arbitrary point $\lambda^{(0)}$ (e.g., the mid-point in the prior distributions), and to calculate the total data likelihood of that point with Eq. (11). The second step is to generate a candidate point $\lambda^{(\text{new})}$ according to a proposal density $P(\lambda^{(\text{new})} \mid \lambda^{(k-1)})$. Point $\lambda^{(\text{new})}$ is accepted or rejected against the Metropolis criterion. Thus, a chain of accepted parameter values and corresponding simulation results are generated. The Bayesian calibration procedure was written in the computer programming language Matlab 7.3 (MatWorks Inc., Natick, MA, USA). We ran at least three parallel MCMC chains with 30,000 iterations each, evaluated the chains for convergence, and thinned the chains (every 20th iteration) when appropriate to reduce within-chain autocorrelation, thereby producing an independent sample of 3000 values for each parameter from the joint posterior distribution. The parameters of the FvCB model were fitted to gas-exchange data from each leaf. Thus, 9000–12,000 values of each parameter for each month were obtained, from which the posterior mean and 95% confidence intervals (CIs: i.e., 2.5th and 97.5th percentiles) can be obtained.

To optimize the parameters of the BWB sub-model (m and g_{swmin}), a linear least-squares optimization procedure was used based on the diurnal and seasonal gas-exchange data of the net assimilation rate, relative humidity and CO_2 concentration at the leaf surface.

Evaluation of model predictions

Model goodness-of-fit was evaluated by using the coupled model to predict net CO_2 assimilation and transpiration rates, which could then be compared with measured values. If the model perfectly predicted the data, all observed-versus-predicted points would lie exactly on the 1:1 line. We also used the root mean square error (RMSE) to characterize the mismatch of the calculated values against the observed values. The RMSE is given by

$$\text{RMSE} = \sqrt{\frac{1}{n}\sum_{i=1}^{n}(f(x_i;\,\lambda) - y_i)^2} \quad (12)$$

where simulations $f(x_i;\,\lambda)$ were calculated using either the posterior expectancy of parameters ($\bar{\lambda}$) or the maximum a posteriori (MAP) estimate of parameters (λ_{MAP}), which is the single best value of the parameter vector in each MCMC chain with a maximal posterior probability distribution (Van Oijen et al. 2005). The posterior mean of predictions was defined as the expectancy of simulations for which parameters were selected from the posterior PDFs.

Results

Environmental conditions

Detailed information on the seasonality of key environmental variables is essential to assess seasonal variation in leaf photosynthesis and stomatal conductance model parameters. Figure 2 shows the seasonal change in daily maximum air temperature ($T_{air\text{-}max}$), daily minimum air temperature ($T_{air\text{-}min}$), daytime mean VPD, precipitation and volumetric soil water content (θ_v). During the growing season (Days 120–275), $T_{air\text{-}max}$ increases markedly from moderate (~20 °C) in late spring (~Day 121) to extreme (>40 °C) by late summer (Day 244)

Table 1. The prior probability distribution is defined as multivariate normal. Median and 95% CIs (i.e., 2.5th and 97.5th percentiles) for photosynthesis parameter values are derived from the literature; n/a indicates that information was not available in the literature. The posterior parameter distributions estimated by MCMC are based on different season and multi-dataset, and are characterized by the mean and 95% CI.

Parameter	Prior probability distribution		Posterior probability distribution					
	Median (95% CI)	References	Mean (95% CI)					
			May	Jun	Jul	Aug	Sep	Multi-data
V_{cmax25} (μmol m^{-2} s^{-1})	62.3 (34.3, 200)	Medlyn et al. (2002), Kosugi and Matsuo (2006), Kattge and Knorr (2007)	51.16 (47.39, 54.92)	63.61 (60.39, 72.20)	112.20 (105.98, 114.07)	72.03 (63.60, 76.24)	58.48 (56.36, 62.03)	70.12 (63.25, 79.24)
J_{max25} (μmol m^{-2} s^{-1})	110.05 (62.3, 179.0)	Medlyn et al. (2002), Kattge and Knorr (2007)	93.66 (90.48, 96.06)	150.73 (145.58, 160.58)	157.41 (150.07, 179.21)	119.11 (111.42, 122.41)	72.68 (62.82, 83.36)	150.32 (133.54, 154.17)
R_{d25} (μmol m^{-2} s^{-1})	1.75 (0.01, 5)	Kosugi et al. (2003), Kosugi and Matsuo (2006)	3.18 (3.02, 3.44)	2.10 (1.85, 2.21)	0.81 (0.71, 0.92)	0.29 (0.28, 0.30)	0.70 (0.66, 0.75)	1.70 (0.98, 2.56)
g_{m25} (μmolm^{-2}s^{-1} Pa^{-1})	2.5 (0.03, 30)	Ethier and Livingston (2004), Sharkey et al. (2007)	6.63 (3.97, 6.72)	8.85 (4.74, 12.09)	9.31 (7.03, 12.00)	8.03 (7.07, 9.87)	7.31 (3.79, 9.30)	8.93 (5.65, 10.34)
K_{c25} (Pa)	27.24 (24.8, 47.03)	Von Caemmerer et al. (1994), Sharkey et al. (2007), Patrick et al. (2009*a*)	27.21 (27.13, 28.39)	27.29 (25.76, 29.03)	27.07 (26.98, 28.99)	27.17 (26.71, 28.78)	27.26 (25.60, 29.36)	27.20 (27.02, 30.00)
K_{o25} (kPa)	16.58 (15.8, 50.4)	Von Caemmerer et al. (1994), Sharkey et al. (2007), Patrick et al. (2009*a*)	16.47 (15.21, 17.79)	16.49 (15.42, 18.32)	16.94 (15.94, 18.18)	16.52 (15.37, 18.60)	16.40 (14.22, 19.65)	16.50 (12.60, 17.95)
Γ^*_{25} (Pa)	3.74 (3.30, 4.85)	von Caemmerer et al. (1994), Sharkey et al. (2007), Patrick et al. (2009*a*)	3.52 (3.45, 3.84)	3.56 (3.46, 3.76)	3.60 (3.27, 3.63)	3.54 (3.45, 3.69)	3.50 (3.30, 3.82)	3.55 (3.42, 3.84)
E_V (kJ mol^{-1})	65.4 (51.3, 128.4)	Leuning (1997), Leuning (2002), Medlyn et al. (2002), Kattge and Knorr (2007), Sharkey et al. (2007), Patrick et al. (2009*a*)	72.50 (61.12, 80.11)	65.23 (60.91, 70.86)	55.54 (47.57, 65.72)	64.56 (53.07, 66.30)	83.36 (81.36, 98.26)	65.01 (43.78, 66.32)
E_J (kJ mol^{-1})	46.08 (35.9, 105.6)	Leuning (1997), Leuning (2002), Medlyn et al. (2002), Kattge and Knorr (2007), Sharkey et al. (2007), Patrick et al. (2009*a*)	62.01 (55.75, 73.11)	55.2 (50.98, 58.47)	47.34 (45.12, 49.24)	64.08 (59.20, 71.70)	48.25 (45.66, 54.26)	60.80 (36.34, 63.96)
E_{Rd} (kJ mol^{-1})	63.9 (41.1, 92.6)	Bernacchi et al. (2001), Ethier and Livingston (2004), Sharkey et al. (2007)	63.22 (49.39, 75.52)	62.84 (53.89, 80.42)	64.09 (62.24, 75.61)	63.84 (59.36, 64.46)	63.18 (52.19, 79.14)	63.50 (28.14, 116.83)

Continued

Table 1. Continued

Parameter	Prior probability distribution		Posterior probability distribution					
	Median (95% CI)	References	Mean (95% CI)					
			May	Jun	Jul	Aug	Sep	Multi-data
E_{gm} (kJ mol^{-1})	49.6 (n/a,n/a)	Sharkey et al. (2007)	49.68 (44.49, 58.31)	49.79 (49.24, 70.75)	50.37 (21.45, 72.52)	49.75 (41.06, 56.69)	49.42 (41.06, 56.69)	49.78 (39.82, 83.37)
E_{Kc} (kJ mol^{-1})	79.97 (62.80, 92.67)	Von Caemmerer (2000), Kosugi et al. (2003), Ethier and Livingston (2004), Sharkey et al. (2007)	70.29 (67.05, 77.84)	70.27 (67.39, 76.37)	70.44 (68.43, 75.73)	70.33 (59.17, 81.76)	70.22 (57.53, 77.81)	70.26 (58.77, 80.21)
E_{Ko} (kJ mol^{-1})	35.95 (18.52, 37.83)	von Caemmerer (2000), Kosugi et al. (2003), Ethier and Livingston (2004), Sharkey et al. (2007)	29.79 (29.54, 30.66)	29.81 (28.42, 31.28)	29.80 (28.78, 31.20)	29.84 (28.20, 35.52)	29.98 (27.90, 31.76)	29.80 (27.39, 31.60)
$E_{\Gamma*}$ (kJ mol^{-1})	26.8 (23.5, 37.2)	Bernacchi et al. (2001), Ethier and Livingston (2004), Sharkey et al. (2007)	26.53 (22.51, 28.44)	26.88 (26.21, 30.20)	26.84 (24.93, 28.79)	26.41 (26.04, 30.99)	26.68 (24.24, 27.09)	26.79 (21.95, 8.31)
H_v (kJ mol^{-1})	200.0 (191.13, 228.5)	Medlyn et al. (2002), Kattge and Knorr (2007)	195.18 (189.54, 195.91)	202.601 (202.03, 205.66)	196.07 (190.96, 201.58)	195.40 (193.04, 204.31)	199.31 (191.08, 203.74)	195.38 (157.02, 218.00)
H_J (kJ mol^{-1})	200.0 (129.9, 214.7)	Leuning (1997), Kattge and Knorr (2007), Leuning (2002), Medlyn et al. (2002), Patrick et al. (2009*a*)	199.60 (190.24, 231.96)	200.29 (182.22, 210.31)	200.40 (162.11, 206.12)	200.21 (179.68, 239.12)	199.16 (173.34, 223.64)	200.00 (176.52, 228.89)
H_{gm} (kJ mol^{-1})	437.4 (n/a,n/a)	Sharkey et al. (2007)	442.09 (413.89, 453.73)	433.82 (426.87, 446.68)	421.12 (413.06, 434.23)	435.47 (416.35, 451.77)	448.73 (436.62, 476.16)	434.01 (424.88, 446.15)
ΔS_v (kJ mol^{-1} K^{-1})	0.65 (0.41, 1.25)	Leuning (1997), Leuning (2002), Medlyn et al. (2002), Kattge and Knorr (2007)	0.41 (0.39, 0.62)	0.44 (0.43, 0.63)	0.48 (0.48, 0.59)	0.48 (0.44, 0.63)	0.55 (0.50, 0.62)	0.48 (0.47, 0.67)
ΔS_J (kJ mol^{-1} K^{-1})	0.65 (0.41, 1.25)	Leuning (1997), Leuning (2002), Medlyn et al. (2002), Kattge and Knorr (2007)	0.64 (0.56, 0.70)	0.64 (0.53, 0.67)	0.64 (0.53, 0.68)	0.62 (0.50, 0.65)	0.68 (0.53, 0.72)	0.63 (0.56, 0.76)
ΔS_{gm} (kJ mol^{-1} K^{-1})	1.4 (n/a,n/a)	Sharkey et al. (2007)	1.38 (0.85, 1.59)	1.44 (1.40, 1.47)	1.28 (0.76, 1.54)	1.33 (1.07, 1.67)	1.36 (0.75, 1.63)	1.35 (0.86, 1.43)
Q_{tr} (μmol m^{-2} s^{-1})	780.0 (500, 1100)	Kosugi et al. (2003)	996.07 (982.14, 1010.0)	1010.40 (996.16, 1024.64)	1002.01 (990.40, 1013.60)	1018.50 (1012.20, 1024.81)	972.54 (958.40986.68)	1015.54 (981.90, 1017.90)
C_{itr} (Pa)	25.0 (17.2, 45.8)	Ethier and Livingston (2004), Miao et al. (2009), Su et al. (2009)	24.95 (24.79, 25.11)	30.50 (28.71, 32.30)	25.61 (24.05, 27.17)	27.22 (26.77, 27.66)	29.95 (28.11, 31.79)	27.65 (25.64, 29.65)

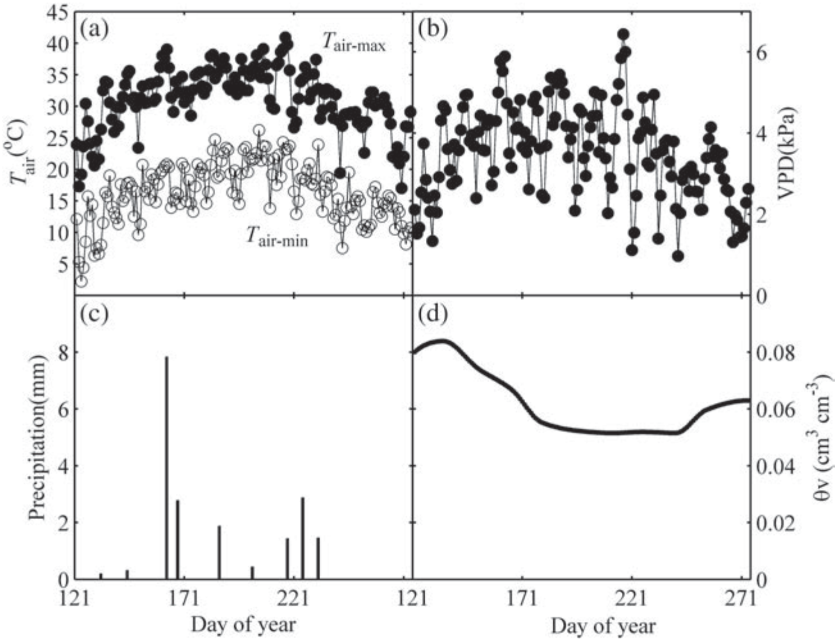

Figure 2. Seasonal variations in daily maximum air temperature ($T_{air\text{-}max}$), minimum air temperature ($T_{air\text{-}min}$), mean daytime air VPD, soil volumetric water content (θ_V) averaged from 0 to 120 cm, and daily precipitation. Mean daytime VPD was for the period between sunrise and sunset. Annual precipitation was 66 mm.

(Figure 2a). $T_{air\text{-}min}$ in the summer varied from 10 to 25 °C, so that leaves experienced a 15–30 °C range in temperature over the course of a day. Leaves experienced great day-to-day variation in daytime mean VPD from 1 to 6 kPa (Figure 2b). Also, half-hour data (not shown) indicated that peak values of VPD as high as 8.5 kPa frequently occurred in the afternoon (~15:00 h).

The year 2008 was relatively abundant in terms of precipitation (66 mm). The maximum rainfall (7.8 mm) was on 12 June (Day 163) and the last rainfall (1.5 mm) was on 20 August (Day 232, Figure 2c). However, it is hard for rainfall to recharge the soil water profile in such an arid area (Zhu et al. 2007). From late spring to summer, the volumetric soil water content slightly decreased and then remained at a steady-state low of about 0.05 cm^3 cm^{-3} (Figure 2d). The reason for this was that water extraction by roots increased as the leaves of plants developed. During autumn when plants withered and daylight hours decreased, a slight increase in soil water content was also found (Figure 2d).

Posterior distribution of the FvCB sub-model parameters

Data obtained under naturally varying conditions in the field, not curves obtained under controlled conditions, were used to parameterize the FvCB model. Thus, preliminary determination of whether a data point in the diurnal course of CO_2 uptake is limited by Rubisco or RuBP regeneration is necessary for deducing biologically meaningful parameter estimations. At current levels of CO_2 (380 µmol mol^{-1}), photosynthesis is commonly Rubisco limited under field conditions (Rogers and Humphries 2000), while RuBP limitation mainly occurred when the photosynthetic quantum flux density (Q) was <700 µmol m^{-2} or the intercellular airspace CO_2 partial pressures (C_i) were >32 Pa (Kosugi et al. 2003). Using these informative priors, our method provided simultaneous estimates of the transition values of Q (Q_{tr}) and C_i (C_{itr}). Specifically, the critical parame-

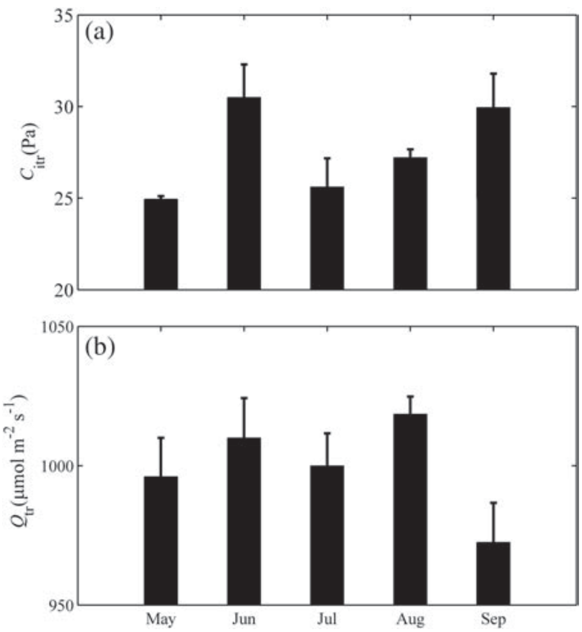

Figure 3. Posterior mean estimates and 95% CIs for (a) the transition intercellular partial pressure of CO_2 (C_{itr}) and (b) photosynthetic quantum flux density (Q_{tr}).

ters C_{itr} and Q_{tr} were assigned according to their PDFs at the beginning of each iterative step. After the iterations, they could be estimated from the MCMC chains generated by the rigorous Bayesian statistical approach. Thus, the Bayesian method allows us to avoid setting fixed and potentially arbitrary transition values of Q and C_i that separate the limitation states of each point in the diurnal curve. The posterior estimates of Q_{tr} and C_{itr} ranged from 972.54 ± 14.13 to 1018.70 ± 6.30 μmol m^{-2} s^{-1} and from 25.61 ± 1.56 to 30.50 ± 1.80 Pa, respectively (Figure 3). Usually, C_{itr} values are manually set at ~20–25 Pa based on work with *Phaesolus vulgaris* (Von Caemmerer and Farquhar 1981). In our study, both Q_{tr} and C_{itr} showed a seasonal variation pattern (Figure 3), and the mean value of C_{itr} determined by our method (C_{itr} = 27.65 Pa) is slightly higher than the empirical value of 20–25 Pa.

Figure 4 shows plots of the posterior parameter distributions corresponding to the means and 95% CIs (i.e., 2.5th and 97.5th percentiles) after calibration with different seasonal dataset and multi-dataset procedures. Such representation makes it possible to visualize seasonal differences in the parameter PDFs, while the shape of the plot reveals the dispersion and symmetry of the marginal distributions (Lehuger et al. 2009). The main photosynthetic parameters (e.g., V_{cmax25}, J_{max25}, R_{d25} and g_{m25}; Figure 4a) and some activation energy parameters (e.g., E_v and E_J; Figure 4b) were updated well by the MCMC procedure, as demonstrated by narrow CIs and seasonal variabilities for these parameters (Figures 4a and b; Table 1). However, this was not the case for other parameters such as K_{c25}, K_{o25}, Γ^*_{25}, E_{Rd}, E_{gm}, E_{Kc}, E_{Ko}, E_{Γ^*}, ΔS_v, ΔS_J, ΔS_{gm}, H_v, H_J and H_{gm}. That is, the posterior means of these parameters were held relatively constant for different seasons with

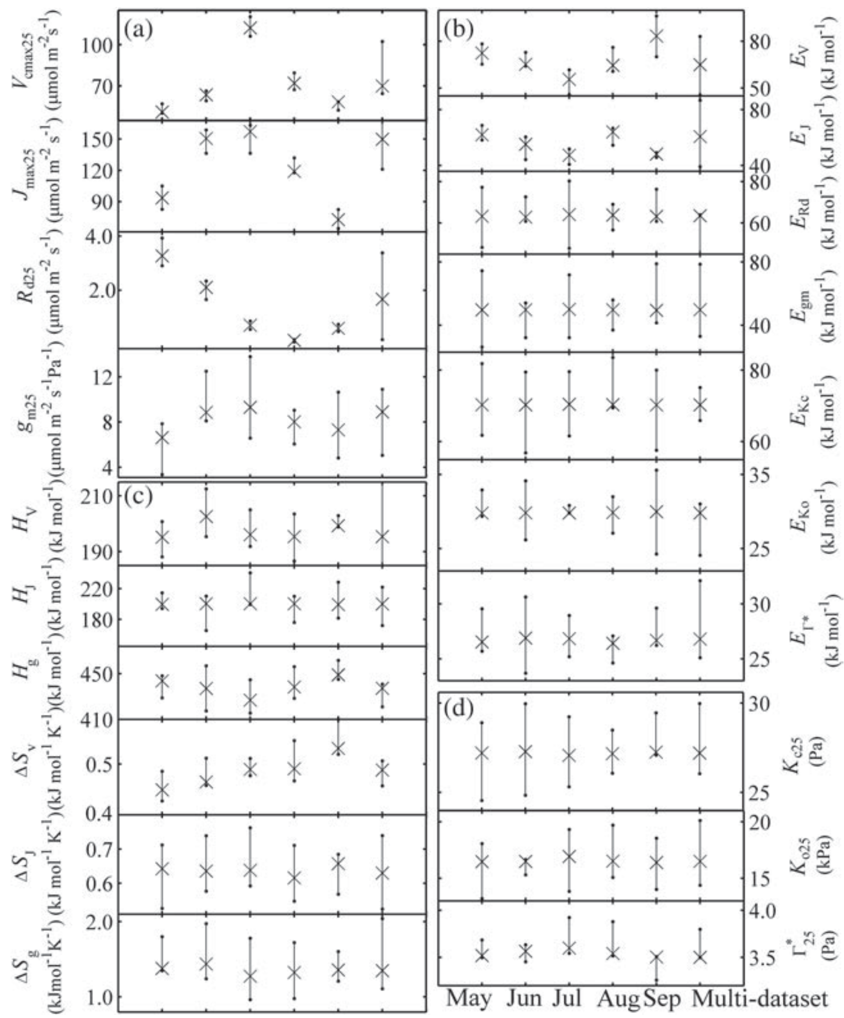

Figure 4. Posterior mean estimates (cross) and 95% CIs (closed circles) for seasonal variation given by the Bayesian approach based on in situ data for (a) the main photosynthetic parameters [maximum rate of carboxylation standardized to 25 °C (V_{cmax25}), maximum rate of electron transport standardized to 25 °C (J_{max25}), mitochondrial respiration standardized to 25 °C (Rd25) and mesophyll conductance standardized to 25 °C (gm25)]; (b) active energy (E_Y); (c) entropy terms (ΔS_Y) and deactivation energy (H_Y); and (d) Michaelis–Menten constant standardized to 25 °C (K_{c25}, K_{o25} and Γ^*_{25}).

relatively broad CIs (Figures 4b–d; Table 1). Also, their posterior means were similar to the means specified by their prior distributions, indicating that these parameters were less identifiable under less informative priors (Patrick et al. 2009*a*). The rightmost plot in each graph in Figure 4 depicts the distribution obtained with the multi-dataset procedure. Its mean value appeared to be more constrained by several seasonal datasets that have similar parameter values, which may be explained by the fact that the combination of such datasets had a comparatively larger number of observations, and subsequently gained more weight in the likelihood function. For example, the mean of V_{cmax25} for the multi-dataset exhibited high similarity to that for June, August and September, and J_{max25} for the multi-dataset seemed to be more contained by June and July (Figure 4a). It was also noticed that the CIs were wider (and thus of higher uncertainty) than those for dataset-by-dataset calibration, owing to the wide ranges covered by the dataset-specific PDFs.

Calibration efficiency of MCMC for the FvCB sub-model

The RMSE between simulated and measured leaf photosynthesis rates was selected as one aspect to describe the calibration efficiency of the MCMC method. Table 2 summarizes the RMSEs obtained with the various parameters updated by MCMC based on different datasets. In the dataset-by-dataset procedure, there were no significant differences in the RMSEs calculated either with simulations using the posterior mean of parameters ($\bar{\lambda}$) or with the posterior mean of predictions generated with the posterior MCMC parameter chains. Thus, the posterior mean parameter values ($\bar{\lambda}$) could be directly used in our coupled CO_2 and H_2O gas-exchange model. We can also notice that the use of the parameter set with maximum posterior probability (λ_{MAP}) can logically improve the RMSEs compared with the use of $\bar{\lambda}$. However, there were no guarantees that λ_{MAP} has realistically biological means. As expected, the multi-dataset calibration was less efficient in reducing the RMSEs than the dataset-by-dataset one (Table 2).

Table 2. RMSEs based on the posterior expectancy of predictions, the posterior expectancy of parameters ($\bar{\lambda}$), the maximum posterior parameters (λ_{MAP}) and the posterior expectancy of parameters from the multi-dataset of the MCMC procedure for the FvCB sub-model using diurnal and seasonal in situ gas-exchange data.

Season	RMSE (in μmol m^{-2} s^{-1}) computed with			
	Posterior expectancy of predictions	Posterior expectancy of parameters	Maximum posterior parameters	Posterior expectancy of parameters from the multi-dataset
May	1.41	1.53	1.45	2.57
June	1.36	1.48	1.42	2.31
July	2.39	2.68	2.46	2.82
August	1.89	2.04	1.91	2.01
September	1.67	1.68	1.66	2.21

Although the RMSEs between the simulations (using $\bar{\lambda}$) and observations were relatively low, caution is still needed to verify that the MCMC method based on the in situ gas-exchange data can yield biologically meaningful estimations of the parameters. Here, the performances of the Bayesian method were compared with the traditional A–C_i curve fitting method (Su et al. 2009) (Supporting Information A1). The results indicated that the main photosynthesis parameters (e.g., V_{cmax25}, J_{max25}, g_{m25}, E_v and E_J) estimated by the two methods were very similar. However, this was not the case for the other parameters. For example, the posterior mean of R_{d25} estimated by the Bayesian method seemed to be about three times that estimated by the A–C_i curve fitting method. Posterior mean values of E_{gm}, E_{Rd}, ΔS_v and ΔS_J estimated by the Bayesian method fell in a narrower range (around their prior distributions) than those estimated by the curve fitting method (Supporting Information A1, Figure S3), which indicated that these parameters were not updated well by the data. However, it should be noticed that ΔS_{gm} estimated by the curve fitting method seems to be unreasonable because four out of the five values continued to be 1. Also, R_{d25} and E_{Rd} in August (Supporting Information A1) were not identified well by the A–C_i curve fitting method. In addition, our updated posterior mean parameter values were verified by previous studies (Zhu et al. 2010). For example, the posterior means of the two main photosynthetic parameters (V_{cmax25} and J_{max25}) in August for *P. euphratica* were close to those estimated by the A–C_i curve fitting method (V_{cmax25} and J_{max25} were 75.09 ± 1.36 and 117.27 ± 2.47 μmol m^{-2} s^{-1}, respectively; Zhu et al. 2010). Thus, it can almost be certain that based on in situ diurnal gas-exchange data, the MCMC method can obtain the biologically meaningful parameters needed in the FvCB sub-model. Potentially, it might be useful in obtaining empirical estimates of the FvCB model parameters and be a complement to the A–C_i curve fitting method in investigating the photosynthetic characteristics of species of interest, especially when the family of A–C_i curves at different temperatures could not be guaranteed.

Stomatal conductance parameters

The relationship between stomatal conductance (g_{sw}; mol m^{-2} s^{-1}) and stomatal index (Ah_s/C_s) of the BWB sub-model of *P. euphratica* is shown in Supporting Information A2 (Figure S1). Table 3 compares the optimized values of the parameters m and g_{swmin} for the BWB sub-model with those of other studies. The results indicated that these parameters varied seasonally. Thus, the assumption of constant parameter values for application of coupled photosynthesis–stomatal conductance models, which are often used as sub-models in

Table 3. List of BWB sub-model parameters optimized by dataset-by-dataset and multi-dataset procedures. A comparison of the parameters with other studies is also given.

Species	Growing season	M	g_{swmin} (mol m^{-2} s^{-1})	r^2	References
P. euphratica	May	15.64	0.032	0.93	This study
	June	11.89	0.016	0.91	This study
	July	13.85	0.218	0.81	This study
	August	17.80	0.079	0.95	This study
	September	27.03	0.003	0.93	This study
	Multi-dataset	18.56	0.039	0.86	This study
Platanus orientalis	May	17.8	0.102	–	Kosugi et al. (2003)
	June to October	9.8	0.061	–	Kosugi et al. (2003)
	November	8.0	0.089	–	Kosugi et al. (2003)
	Multi-dataset	10.7	0.067	–	Kosugi et al. (2003)
Prunus × yedoensis	May	11.5	0.071	–	Kosugi et al. (2003)
	June to October	6.9	0.094	–	Kosugi et al. (2003)
	November	16.1	0.081	–	Kosugi et al. (2003)
	Multi-dataset	7.7	0.093	–	Kosugi et al. (2003)
Liriodendron tulipifera	May	26.1	0.052	–	Kosugi et al. (2003)
	June to October	9.3	0.052	–	Kosugi et al. (2003)
	November	18.9	0.063	–	Kosugi et al. (2003)
	Multi-dataset	9.4	0.064	–	Kosugi et al. (2003)
Gossypium hirsutum (cotton)	–	9.58	0.0811	–	Harley et al. (1992)
Quercus alba and *Acer rubrum*	–	9.5	0.0175	–	Harley and Baldocchi (1995)
Quercus ilex	–	15.0	0.005	–	Sala and Tenhunen (1996)
Quoted and used by SiB2					
C_4 plants	–	4	0.01	–	Sellers et al. (1996)
C_3 plants	–	9	0.01	–	Sellers et al. (1996)
Conifers	–	6	0.01	–	Sellers et al. (1996)

large-scale modeling studies [i.e., SiB2 (Sellers et al. 1996) and LSM (Bonan 1998)], may not be the case. It was also noticed that the pattern of seasonal change for the stomatal conductance parameters differed from that of the photosynthetic parameters (i.e., V_{cmax25} and J_{max25}). For example, relatively large m was observed during the expansion period (May) and the highest value of m occurred in September, as photosynthetic parameters declined (Table 3).

Coupled-model validation

Having parameterized the coupled model as described above (including both dataset-by-dataset and multi-dataset procedures), we simulated the diurnal courses of photosynthesis and transpiration on the leaf scale, using leaf temperature, Q, C_s and h_s as driving variables. Diurnal variations in environmental variables for the measurement days are presented in Supporting Information A3 (Figure S1). The resulting simulations using both dataset-by-dataset and multi-dataset optimized parameters were compared with measured rates of net CO_2 assimilation (Figure 5a) and transpiration (Figure 5b). Not surprisingly, the coupled model produced a better fit to the net assimilation rate for all seasons when dataset-by-dataset optimized parameters were considered. Points in the plots of observed-versus-predicted photosynthesis fell tightly along the 1:1 line ($r^2 = 0.84$, 0.73, 0.98, 0.90 and 0.98 with RMSEs = 1.67, 2.95, 0.41, 0.89 and 1.14 for May to September, respectively; data not shown). The error when using multi-dataset optimized parameters was not negligible during the leaf expansion (May and June) and senescence periods (September). In general, the net assimilation rate was underestimated and overestimated by the multi-dataset procedure during the leaf expansion period and senescence period, respectively (Figure 5a). Thus, for long time simulations of net CO_2 assimilation, it was important to consider the physiological changes in the photosynthetic parameters.

Also, the coupled model optimized by the dataset-by-dataset procedure can capture the trend of diurnal changes of transpiration well (Figure 5b) with $r^2 = 0.90$, 0.81, 0.93, 0.51 and 0.89 and RMSEs = 0.69, 0.89, 0.75, 2.06 and 0.71 for May to September, respectively (data not shown). However, the precision of simulated transpiration rate was less satisfactory for the multi-dataset procedures, and the transpiration was overestimated in June and July and underestimated in September (Figure 5b).

Discussion

Compositive evaluation of the Bayesian approach

Parameter estimation is a critical but complex issue that has not been explicitly addressed in ecosystem modeling (Medlyn

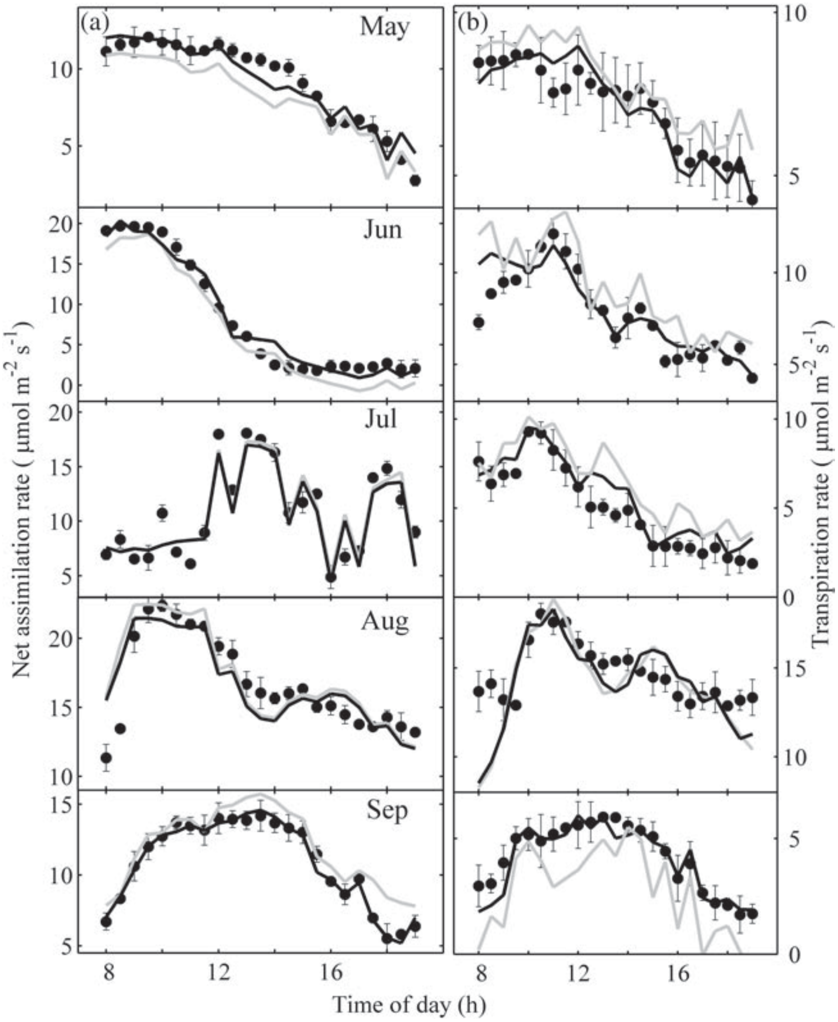

Figure 5. Comparison of the observed (closed circles) and estimated (a) net assimilation rates and (b) transpiration rates using the optimized parameters against separate datasets (black line) or the multi-dataset (gray line).

et al. 2005, Luo et al. 2009). Most of the published studies on ecosystem process models avoid the issue of parameter estimations because of the difficulty in identifying relatively large numbers of parameters against limited sets of data (Luo et al. 2009). In reality, the number of identifiable parameters in any process-based ecosystem model is extremely low for traditional optimizing algorithms (such as Gauss–Newton, steepest descent or Levenberg–Marquardt algorithms). For example, Dubois et al. (2007) show that from given A–C_i data only three (V_{cmax}, J_{max} and R_d) out of the six parameters (V_{cmax}, J_{max}, R_d, K_c, K_o and Γ^*) in the FvCB model can be independently estimated. Wang et al. (2001) showed that a maximum of only four parameters in the canopy photosynthesis model could be estimated independently using eddy-flux data. In contrast, the MCMC method using a conditional-probabilistic approach based on the Bayesian theorem dissects a high-dimensional joint posterior distribution for all unknowns to a collection of low-dimensional conditional distributions and sample alternately (Clark 2005, Janes and Gelfand 2006). In this way, the algorithm marginalizes over the full model, and complex problems are handled like simple ones. Now, the Bayesian method has gained wide acceptance for its potential to accommodate high-dimensional parameter estimation problems [see Clark and Gelfand (2006) for a comprehensive review]. Here, we used a Bayesian framework to couple the FvCB model with diurnal data to simultaneously estimate plant-level variability in kinetic constants, photosynthetic and temperature dependence parameters. The Bayesian analyses of the photosynthesis model parameters can help us achieve two main goals. First, it can improve our biological understanding of plant behavior between seasons and environmental conditions (discussed below). Secondly, it helps us to identify the sensitivity of parameters in modeling purposes. In other words, we can reasonably predict which parameters are to be constant and which parameters are to be time-varying in long-term and large-scale modeling applications (discussed below).

The results indicated that the main photosynthetic parameters (e.g., V_{cmax25}, J_{max25}, g_{m25}, E_v and E_J) estimated by the

Bayesian method and the A–C_i curve fitting method based on different datasets can be very close to one another (Supporting Information A1, Figure S3). However, this was not the case for other parameters (i.e., K_{c25}, K_{o25}, Γ_{25}*, H_v, H_J, H_{gm}, ΔS_v, ΔS_J and ΔS_{gm}). That is, the posterior means of these parameters were mainly constrained by their prior distributions (Supporting Information A1, Figure S3). Thus, eliciting proper prior distributions for these parameters is important to lead to correct scientific inferences (Tyul et al. 2008), and substantial controlled-condition experiments on species of interest are still needed in further studies. Although there were slight differences for some parameters estimated by the two methods, the FvCB sub-model optimized by the Bayesian method based on the dataset-by-dataset procedure successfully reproduced the observation pattern of A–C_i responses at all five seasons with different leaf temperatures (contour lines; Supporting Information A1, Figure S4). The explanation is that these parameters may be relatively constant among C_3 plants, and they were constrained well by the prior distributions informed from previous A–C_i analyses. Therefore, the A–C_i curve fitting methods provided valuable information about the parameter distributions for the Bayesian method. In other words, it would be hard for the Bayesian method to obtain correct estimations of the interested parameter posterior distributions without incorporating 'informed' guesses from the A–C_i analyses.

To date, numerous A–C_i curves covering broad-leaved trees and shrubs, needle-leaved (coniferous) trees, grasses and other herbaceous plants at different temperatures varying from 5 to 40 °C have been measured (Wullschleger 1993, Wohlfahrt et al. 1999, Medlyn et al. 2002, Kattge and Knorr 2007) to derive the photosynthetic performance of intact leaves. However, using diurnal gas-exchange data to estimate the photosynthetic parameters has not received much attention (but see Kosugi et al. 2003, Gao et al. 2004). Kosugi et al. (2003) pointed out that by using in situ data one can derive much more information than by examining the A–C_i curve obtained with a controlled chamber. Here, we thought that the Bayesian method coupled with the diurnal gas-exchange data could be a good complement to the A–C_i curve fitting method to investigate photosynthetic characteristics, especially when the family of A–C_i curves at different temperatures, which is very time-consuming and equipment-intensive, could not be guaranteed. What is the reason that the diurnal data can be used by the Bayesian method to parameterize the photosynthetic model? The explanation may be that both the environmental variables (e.g., Q, leaf temperature) and C_i showed relatively large variations during a diurnal course; thus the daily net CO_2 assimilation rate was limited by different photosynthetic processes. Taking advantage of the Bayesian method, the critical parameters C_{itr} and Q_{tr} used to differentiate between Rubisco and RuBP limitation were simultaneously identified. Therefore, each CO_2 gas-exchange data point includes information on either the Rubisco-limited process [Eq. (2)] or the RuBP-limited process [Eq. (3)], and related parameters can be informed by the corresponding points. Thus, the Bayesian method provided us with the potential to sufficiently use the diurnal data to derive the photosynthetic characteristics of species of interest. Also, the parameters estimated from in situ gas-exchange data were considered to be the 'actual' response of leaves in field conditions.

Seasonal variations of the coupled-model parameters

The two main parameters representing photosynthetic capacity, V_{cmax25} and J_{max25}, have been observed to change seasonally in our research. For example, the maximum values of both V_{cmax25} and J_{max25} occurred in July and declined after that (Figure 4a). Seasonal variabilities of V_{cmax25} and J_{max25} have also been shown to occur in both deciduous (Wilson et al. 2000, Kosugi et al. 2003) and coniferous trees (Medlyn et al. 2002). The seasonal fluctuation of V_{cmax25} and J_{max25} seems to correspond to the seasonal changes in leaf nitrogen content N_{area} (g m^{-2}), and the linear correlations between them were strong (Figure 6). Evidence has shown that peaked functions were necessary to describe the temperature response of J_{max} and V_{cmax} for desert plants, which are often exposed to hot and highly variable temperature (Patrick et al. 2009*a*). Some studies suggested that the peaked function is over-parameterized,

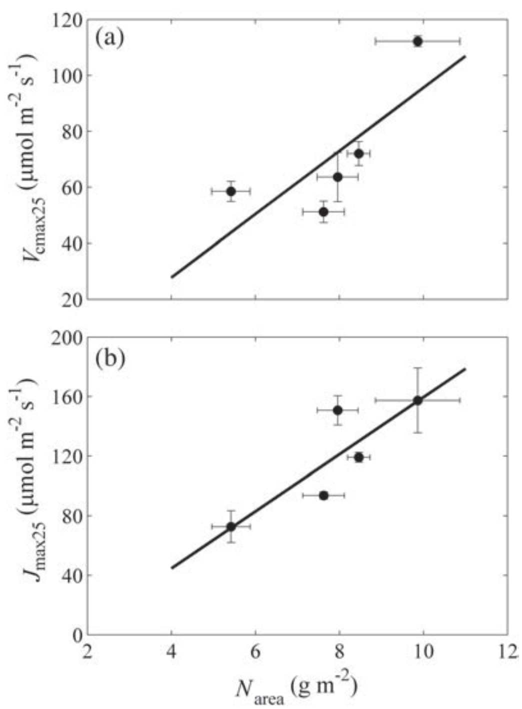

Figure 6. (a) Maximum rate of Rubisco activity standardized to 25°C (V_{cmax25}) and (b) potential electron transport rate standardized to 25 °C (J_{max25}), as a function of leaf nitrogen content. Equations for regression lines: $V_{cmax25} = 11.31N_{area} - 17.49$, $r^2 = 0.58$; $J_{max25} = 19.15N_{area} - 31.95$, $r^2 = 0.73$.

thereby increasing the difficulty of estimating photosynthesis parameters (Harley et al. 1992, Dreyer et al. 2001, June et al. 2004). In order to reduce the number of parameters, several investigators used fixed values for the deactivation energy (i.e., H_v and H_J at 200 kJ mol^{-1}; Medlyn et al. 2002) and the entropy term (i.e., ΔS_v and ΔS_J at 0.65 kJ mol^{-1} K^{-1}; Xu and Baldocchi 2003). We thought it was acceptable because the posterior estimates of the deactivation energy were constrained by the prior distribution. As for activation energy (E_Y), a proper estimation is necessary to investigate the mechanisms underlying photosynthetic temperature acclimation. This study confirms that the optimum temperature (T_{opt}) of V_{cmax} and J_{max} increased with ambient temperature (Figure 7). It was noticed that the T_{opt} of V_{cmax} and J_{max} for *P. euphratica* is larger than that for the 18 broad-leaved trees and shrubs reported by Kattge and Knorr (2007), ranging between 26.6 and 50.9 °C and between 19.2 and 44.5 °C, respectively. This seems to be due to the fact that the growth temperature of *P. euphratica* (mean 23 °C during the growing season) is relatively high compared with the 18 species in Kattge and Knorr's list (ranging between 11 and 20 °C). However, a similar large value of T_{opt} (50.86 °C) for the desert plant *Tidestromia oblongifolia* was reported by Berry and Raison (1981).

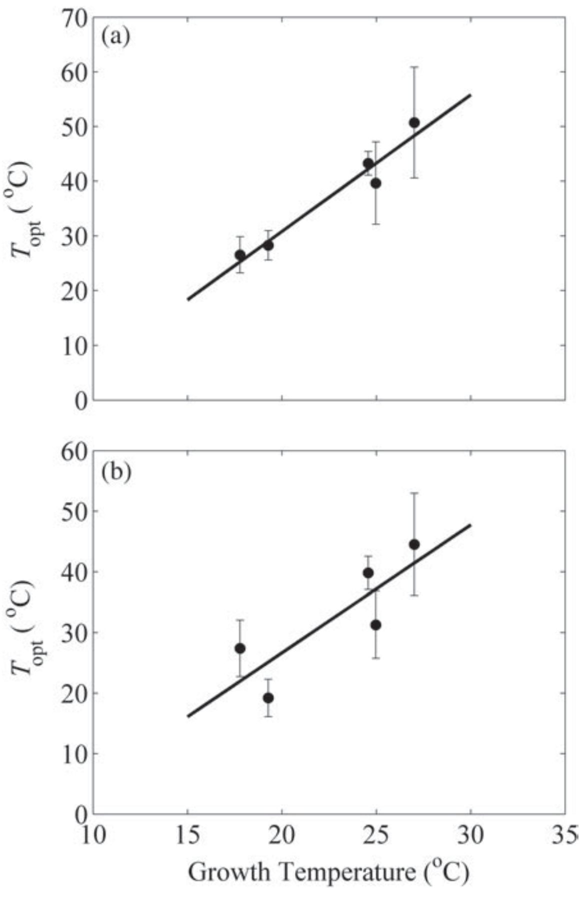

Figure 7. Relationship between optimal temperature and 15-day average growing ambient temperature prior to measurement: (a) V_{cmax} vs. growth temperature and (b) J_{max} vs. growth temperature. Regression equations: V_{cmax}: $T_{opt} = 2.50T_{growth} - 19.02$, $r^2 = 0.95$; J_{max}: $T_{opt} = 2.11T_{growth} - 15.56$, $r^2 = 0.70$.

Many studies have shown that the traditional A–C_i curve fitting methods have had difficulty in obtaining accurate or biologically realistic estimates of R_{d25} (but see Dubois et al. 2007, Sharkey et al. 2007, Su et al. 2009), and, as such, R_{d25} is sometimes not reported (Medlyn et al. 2002). However, Patrick et al. (2009*a*) showed that if both A–C_i and A–Q curves were used simultaneously, estimates of R_{d25} were positive and therefore more biologically realistic. This implies that assimilating the information of photosynthetic quantum flux density (Q) will improve the estimations of R_d. In field conditions, the diurnal course of Q showed a wide variation, and provided valuable information to estimate R_d. The posterior means for R_{d25} estimated by the Bayesian method were on average $0.02 \times V_{cmax25}$ (Table 1) and were consistent with the relationship used by some photosynthetic models (i.e., R_{d25} was set at 0.01–0.02 × V_{cmax25}; Von Caemmerer 2000, Bernacchi et al. 2001, Warren and Dreyer 2006). However, R_{d25} estimated by the A–C_i curve fitting method was only two-fifths of that estimated by the Bayesian method (Supporting Information A1, Figure S3). Thus, the values of R_{d25} estimated by the A–C_i curve fitting method seemed to be slightly lower.

The kinetic properties of Rubisco (K_c, K_o and Γ^*) were relatively constant during the growing season (Figure 4d). Medlyn et al. (2002) reported that values of V_{cmax} and J_{max} derived from gas-exchange data depend strongly on the assumed values of K_c, K_o and Γ^*. Thus, there is a need for more information on the temperature dependence of K_c, K_o and Γ^*. Unfortunately, few modeling studies have estimated the temperature dependence of these parameters because of the difficulty in collecting field data directly related to these parameters. Here, we did not assume constant values for the kinetic constants or the temperature response parameters, but rather used informative priors to account for variability, thereby obtaining more accurate estimates for parameters directly related to V_{cmax} and J_{max}.

Our study indicated that leaf development and aging to some extent affect g_{m25}. During leaf development from unfolding to maturation, the posterior mean of g_{m25} slightly increases in parallel with leaf photosynthetic capacity. In contrast, leaf aging results in some decreased g_{m25} (Figure 4a). However, it should be noticed that the temperature response parameters of g_m were poorly informed by the field measurement data. This may be due to two main reasons. The first one is that in addition to temperature g_m has been shown to be affected by other environmental factors such as VPD, soil water, leaf structure and nutrient deficits (Flexas et al. 2008, Niinemets et al. 2009*b*). Thus, further study of the effect of environmental variation on g_m is needed to correctly parameterize temperature dependency functions of g_m. The second one is that g_m changes rapidly in response to varying C_i (Flexas et al. 2007, Niinemets et al. 2009*b*). Therefore, this should be taken into account for correct parameterization of the FvCB model (Niinemets et al. 2009*a*). At present, more studies are urgently needed to find a proper function to describe the behavior of g_m in response to varying CO_2 (Flexas et al. 2007, Niinemets et al. 2009*a*, Su et al. 2009).

As to the stomatal conductance model, it seems to be more proper to take the seasonal variation of m and g_{swmin} into consideration in the long-term simulation of gas exchange. Some studies have reported that m becomes small during soil drought conditions (Sala and Tenhunen 1996, Kirschbaum 1999, Tuzet et al. 2003). However, direct examination of the relationship between photosynthesis and stomatal conductance on *Pinus ponderosa* found that g_{swmin} rather than m was related to soil moisture potential (Misson et al. 2004). In this study, we found that parameters m and g_{swmin} were very strongly correlated. For example, low values in m during the summer season (i.e., June and July; Table 3) were compensated by relatively large g_{swmin}. Thus, it could be questioned whether only one parameter of the BWB model could be used as the indicator of soil drought condition. This state may arise because the BWB model is empirical and phenomenological in nature. Therefore, mechanistic stomatal models (i.e., Gao et al. 2003) with biologically meaningful parameters are urgently needed. Also, lack of a mechanistic basis for using h_s in the BWB model has been criticized, and it was suggested that h_s be replaced by VPD (Lloyd 1991). Leuning et al. (1995) modified the BWB model by replacing h_s with VPD to allow for low intercellular CO_2 concentration by using $(C_s - \Gamma)$ in the denominator so that the data when $A \to 0$ could be included, where Γ is the CO_2 compensation point of assimilation in the presence of dark respiration. We also tested a coupled model incorporating the Leuning model for *P. euphratica* and found that it performed similarly to the BWB model (data not shown).

Recommendations for long-term and large-scale applications

The study has two major implications for modeling of the long-term carbon and water cycle in forest canopy models. First, the similarities between the posterior and prior distributions for kinetic properties (K_{c25}, K_{o25}, Γ^*_{25}, E_{Kc}, E_{Ko} and E_{Γ^*}), entropy terms (ΔS_v, ΔS_J and ΔS_{gm}) and deactivation energy (H_v, H_J and H_{gm}) indicated that these parameters can be considered to be constant for modeling purposes. In contrast, it seems to be more reasonable to take the seasonal variations of the main photosynthetic parameters (i.e., V_{cmax25}, J_{max25}, R_{d25}, g_{m25}, E_v and E_J) into account for long-term modeling applications. Large seasonal variations in photosynthetic capacity (i.e., V_{cmax}, J_{max} and R_d) could mostly be explained by changes in leaf nitrogen content and high ambient temperature. Thus, a function of ambient temperature or of foliar nitrogen content should be used to describe the seasonal variations of the photosynthetic capacity parameters (Medlyn et al. 2002). Also, it was noticed that both m and g_{wmin} changed seasonally and were strongly correlated, which is the problem of the BWB sub-model itself. Overall, the coupled model using dataset-by-dataset optimized parameters can successfully reproduce the observed CO_2 and H_2O exchange process.

Secondly, our study indicated that parameters estimated by the Bayesian method based on diurnal gas-exchange data were similar to that by the traditional A–C_i curve fitting method. As canopy-scale CO_2 fluxes are the integral representation of the individual leaf-scale photosynthesis process, eddy covariance measurements can thus be used to obtain biologically meaningful parameter estimates of terrestrial ecosystem models for the carbon cycle. This was also illustrated by the growing number of studies focused on parameterization of various process-based carbon cycle models using eddy covariance measurements (Wang et al. 2001, Knorr and Kattge 2005, Braswell et al. 2005, Williams et al. 2005, Sacks et al. 2006). However, there is still much to learn about the differences in parameters determined by data at different scales (e.g., leaf-scale and canopy-scale), and the mechanistic correlation between them.

Conclusions

This study applied a coupled model to simulate CO_2 and H_2O fluxes at the leaf scale using data obtained from in situ leaf-scale observations of the diurnal and seasonal changes in the CO_2 and H_2O fluxes of a typical desert wood species. The Bayesian approach using in situ gas-exchange data and not the A–C_i curves can provide us with a fully parameterized photosynthesis model, which might be with a complement to the A–C_i curve fitting method and useful for long-term simulation of carbon assimilation on the leaf, canopy, regional and terrestrial scales. Moreover, insight into the seasonal trends in photosynthesis and stomatal conductance parameters will improve our understanding of the underlying physiological mechanism. Finally, predictions of the coupled model using parameters calibrated by the multi-dataset were less satisfactory than those calibrated against separate datasets, which indicated that the impact of seasonal fluctuations of leaf physiology should be incorporated in models of carbon and water uptake of desert broad-leaved forests.

Acknowledgments

The authors thank Dr Zongqiang Chang and Dr Shengkui Cao for their help with field observation, and Dr Meng Gao and Dr Yingcun Ge for improving the figure quality of the manuscript. We would like to thank Prof. Ram Oren (Editor-in-Chief) and Prof. Ülo Niinemets (Editor) for critical comments and edits on an earlier draft of the manuscript. We also thank the two anonymous reviewers for their critical reviews and helpful comments.

Funding

This research was supported by National Natural Science Foundation of China (Nos. 40925004, 40771036, 41001242 and 40701054), the national high-tech program (863) project ‘a common software for multi-source remote sensing data assimilation’ (grant number: 2009AA12Z130).

Supplementary data

Supplementary data for this article are available at *Tree Physiology* online.

References

Ball, J.T., I.E. Woodrow and J.A. Berry. 1987. A model predicting stomatal conductance and its contribution to the control of photosynthesis under different environmental conditions. *In* Progress in Photosynthesis Research. Ed. I. Biggins. Martinus Nijhoff Publishers, Dordrecht, The Netherlands, pp 221–224.

Bernacchi, C.J., E.L. Singsaas, C. Pimentel, A.R. Portis and S.P. Long. 2001. Improved temperature response functions for models of Rubisco-limited photosynthesis. Plant, Cell Environ. 24:253–259.

Berry, J.A. and J.K. Raison. 1981. Response of macrophytes to temperature. *In* Encyclopedia of Plant Physiology. Eds. Lange, O.L., P.S. Nobel, C.B. Osmond and H. Ziegler. Springer, Berlin, Germany, pp 277–338.

Bonan, G.B. 1998. The land surface climatology of the NCAR land surface model coupled to the NCAR Community Climate Model. J. Climate 11:1307–1326.

Braswell, B.H., W.J. Sacks, E. Linder and D.S. Schimel. 2005. Estimating diurnal to annual ecosystem parameters by synthesis of a carbon flux model with eddy covariance net ecosystem exchange observations. Global Change Biol. 11:335–355.

Cable, J.M., K. Ogle, D.G. Williams, J. Weltzin and T.E. Huxman. 2008. Soil texture drives responses of soil respiration to precipitation pulses in the Sonoran Desert: implications for climate change. Ecosystems 11:961–979.

Cable, J.M., K. Ogle, A.P. Tyler, M.A. Pavao-Zuckerman and T.E. Huxman. 2009. Woody plant encroachment impacts on soil carbon and microbial processes: results from a hierarchical Bayesian analysis of soil incubation data. Plant Soil 320:153–167.

Clark, J.S. 2005. Why environmental scientists are becoming Bayesians. Ecol. Lett. 8:2–14.

Clark, J.S. and A.E. Gelfand. 2006. A future for models and data in environmental science. Trends Ecol. Evol. 12:375–380.

Collatz, G.J., J.T. Ball, C. Grivet and J.A. Berry. 1991. Physiological and environmental regulation of stomatal conductance, photosynthesis and transpiration: a model that includes laminar boundary layer. Agric. Forest Meteorol. 54:107–136.

Dreyer, E., R.X. Le, P. Montpied, F.A. Daudet and F. Masson. 2001. Temperature response of leaf photosynthetic capacity in seedlings from seven temperate tree species. Tree Physiol. 21:223–232.

Dubois, J.J.B., E.L. Fiscus, F.L. Booker, M.D. Flowers and C.C. Reid. 2007. Optimizing the statistical estimation of the parameters of the Farquhar–von Caemmerer–Berry model of photosynthesis. New Phytol. 176:402–414.

Ethier, G.T. and N.J. Livingston. 2004. On the need to incorporate sensitivity to CO_2 transfer conductance in to the Farquhar–von Caemmerer–Berry leaf photosynthesis model. Plant, Cell Environ. 27:137–153.

Farquhar, G.D., S. von Caemmerer and J.A. Berry. 1980. A biochemical model of photoshynthetic CO_2 assimilation in leaves of C_3 species. Planta 149:78–90.

Flexas, J., A. Diaz-Espejo, J. Galmes, R. Kaldenhoff, H. Medrano and M. Ribas-Carbo. 2007. Rapid variations of mesophyll conductance in response to changes in CO_2 concentration around leaves. Plant, Cell Environ. 30:1284–1298.

Flexas, J., R.C. Miquel, D.E. Antonio, G. Jeroni and H. Medrano. 2008. Mesophyll conductance to CO_2: current knowledge and future prospects. Plant, Cell Environ. 31:602–621.

Gao, Q., P. Zhao, X. Zeng, X. Cai and W. Shen. 2003. A model of stomatal conductance to quantify the relationship between leaf transpiration, microlimate and soil water stress. Plant, Cell Environ. 25: 1373–1381.

Gao, Q., X.S. Zhang, Y.M. Huang and H.M. Xu. 2004. A comparative analysis of four models of photosynthesis for 11 plant species in the Loess plateau. Agric. Forest Meteorol. 126:203–222.

Gedney, N., P.M. Cox, R.A. Betts, O. Boucher, C. Huntingford and P.A. Stott. 2006. Detection of a direct carbon dioxide effect in continental river runoff records. Nature 439:835–838.

Gelfand, A.E. and A.F.M. Smith. 1990. Sampling-based approaches to calculating marginal densities. J. Am. Stat. Assoc. 85:398–409.

Gelman, A. and D.B. Rubin. 1992. Inference from iterative simulation using multiple sequences. Stat. Sci. 7:457–511.

Gordon, W.S. and J.S. Famiglietti. 2004. Response of the water balance to climate change in the United States over the 20th and 21st centuries: results from the VEMAP Phase 2 model intercomparisons. Global Biogeochem. Cycles 18:GB1030, doi:10.1029/2003GB002098

Harley, P.C. and D.D. Baldocchi. 1995. Scaling carbon dioxide and water vapour exchange from leaf to canopy in a deciduous forest. I. Leaf model parametrization. Plant, Cell Environ. 18:1146–1156.

Harley, P.C., J.D. Tenhunen and O.L. Lange. 1986. Use of an analytical model to study limitation on net photosynthesis in *Arbutus unedo* under field conditions. Oecologia 70:393–401.

Harley, P.C., R.B. Thomas, J.F. Reynolds and B.R. Strain. 1992. Modeling photosynthesis of cotton grown in elevated CO_2. Plant, Cell Environ. 15:271–282.

Hastings, W.K. 1970. Monte Carlo sampling methods using Markov chains and their applications. Biometrika 57:97–109.

Hatton, T.J., J. Walker, W.R. Dawes and F.X. Dunin. 1992. Simulations of hydroecological responses to elevated CO_2 at the catchment scale. Aust. J. Bot. 40:679–696.

Janes, S.C. and A.E. Gelfand. 2006. A future for models and data in environmental science. Trends Ecol.Evol. 21:375–380.

June, T., J.R. Evans and G.D. Farquhar. 2004. A simple new equation for the reversible temperature dependence of photosynthetic electron transport: a study on soybean leaf. Funct. Plant Biol. 31:275–283.

Kattge, J. and W. Knorr. 2007. Temperature acclimation in a biochemical model of photosynthesis: a reanalysis of data from 36 species. Plant, Cell Environ. 30:1176–1190.

Kirschbaum, M.U.F. 1999. CenW, a forest growth model with linked carbon, energy, nutrient and water cycles. Ecol. Model. 118:17–59.

Knorr, W. and J. Kattge. 2005. Inversion of terrestrial ecosystem model parameter values against Eddy covariance measurements by Monte Carlo sampling. Global Change Biol. 11:1333–1351.

Kosugi, Y. and N. Matsuo. 2006. Seasonal fluctuations and temperature dependence of leaf gas exchange parameters of co-occurring evergreen and deciduous trees in a temperate broad-leaved forest. Tree Physiol. 26:1173–1184.

Kosugi, Y., S. Shibata and S. Kobashi. 2003. Parameterization of the CO_2 and H_2O gas exchange of several temperate deciduous broad-leaved trees at the leaf scale considering seasonal changes. Plant, Cell Environ. 26:285–301.

Lasch, P., F.W. Badeck, F. Suckow, M. Lindner and P. Mohr. 2005. Model-based analysis of management alternatives at stand and regional level in Brandenburg (Germany). For. Ecol. Manage. 207:59–74.

Lehuger, S., B. Gabriellea, M. van Oijenb, D. Makowskic, J.C. Germond, T. Morvane and C. Hénaultd. 2009. Bayesian calibration of the nitrous oxide emission module of an agro-ecosystem model. Agric., Ecosyst. Environ. 133:208–222.

Leuning, R. 1997. Scaling to a common temperature improves the correlation between the photosynthesis parameters J_{max} and V_{cmax}. J. Exp. Bot. 48:345–347.

Leuning, R. 2002. Temperature dependence of two parameters in a photosynthesis model. Plant, Cell Environ. 25:1205–1210.

Leuning, R., F.M. Kelliher, D.G.G. de Pury and E.D. Schulze. 1995. Leaf nitrogen, photosynthesis, conductance and transpiration: scaling from leaves to canopies. Plant, Cell Environ. 18:1183–1200.

Lloyd, J. 1991. Modeling stomatal response to environment in *Macadamia integrifolia*. Austral. J. Plant Physiol. 18:649–660.

Long, S.P., W.F. Postl and H.R.B. Nordenkampf. 1993. Quantum yields for uptake of carbon dioxide in C_3 vascular plants of contrasting habitats and taxonomic groupings. Planta 189:226–234.

Luo, Y.Q., E.S. Weng, X.W. Wu, C. Gao, X.H. Zhou and L. Zhang. 2009. Parameter identifiability, constraint, and equifinality in data assimilation with ecosystem models. Ecol. Appl. 19:571–574.

Medlyn, B.E., D. Loustau and S. Delzon. 2002. Temperature response of parameters of a biochemically based model of photosynthesis. I. Seasonal changes in mature maritime pine (*Pinus pinaster* Ait.). Plant, Cell Environ. 25:1155–1165.

Medlyn, B.E., A.P. Robinson, R. Clement and R.E. McMurtrie. 2005. On the validation of models of forest CO_2 exchange using eddy covariance data: some perils and pitfalls. Tree Physiol. 25:839–857.

Metropolis, N.R., A.W. Rosenbluth, M.N. Rosenbluth and A.H. Teller. 1953. Equations of state calculations by fast computing machines. J. Chem. Phys. 21:1087–1091.

Miao Z.W., M. Xu, J.R. Lathrop and Y.F. Wang. 2009. Comparison of the A–C_c curve fitting methods in determining maximum ribulose 1.5-bisphosphate carboxylase/oxygenase carboxylation rate, potential light saturated electron transport rate and leaf dark respiration. Plant, Cell Environ. 32:109–122.

Misson, L., J.A. Panek and A.H. Goldstein. 2004. A comparison of three approaches to modeling leaf gas exchange in annually drought-stressed ponderosa pine forests. Tree Physiol. 24:529–541.

Morales, P., M.T. Sykes, I.C. Prentice et al. 2005. Comparing and evaluating process-based ecosystem model predictions of carbon and water fluxes in major European forest biomes. Global Change Biol. 11:2211–2233.

Niinemets, Ü. and D. Tenhunen. 1997. A model separating leaf structural and physiological effects on carbon gain along light gradients for the shade-tolerant species *Acer saccharum*. Plant, Cell Environ. 20:845–866.

Niinemets, Ü., O. Kull and J.D. Tenhunen. 1998. An analysis of light effects on foliar morphology, physiology, and light interception in temperature deciduous woody species of contrasting shade tolerance. Tree Physiol. 18:681–696.

Niinemets, Ü., E. Sonninen and M. Tobias. 2004. Canopy gradients in leaf intercellular CO_2 mole fractions revised: interactions between leaf irradiance and water stress need consideration. Plant, Cell Environ. 27:569–583.

Niinemets, Ü., D.E. Antonio, J. Flexas, J. Galmés and C.R. Warren. 2009*a*. Importance of mesophyll diffusion conductance in estimation of plant photosynthesis in the field. J. Exp. Bot. 60:2271–2282.

Niinemets, Ü., I.J. Wright and J.R. Evans. 2009*b*. Leaf mesophyll diffusion conductance in 35 Australian sclerophylls covering a broad range of foliage structural and physiological variation. J. Exp. Bot.60:2433–2449.

Nogues, S. and L. Alegre. 2002. An increase in water deficit has no impact on the photosynthetic capacity of field-grown Mediterranean plants. Funct. Plant Biol. 29:621–630.

Ogle, K. and J.J. Barber. 2008. Bayesian data-model integration in plant physiological and ecoystem ecology. Progr. Bot. 69:281–311.

Ogle, K., J.B. Jarrett, W. Cynthia and T. Brenda. 2009. Hierarchical statistical modeling of xylem vulnerability to cavitation. New Phytol. 182:541–554.

Patrick, L.D., K. Ogle and D.T. Tissue. 2009*a*. A hierarchical Bayesian approach for estimation of photosynthetic parameters of C_3 plants. Plant, Cell Environ. 32:1695–1709.

Patrick, L.D., K. Ogle, C.W. Bell, J. Zak and D. Tissue. 2009*b*. Physiological responses of two contrasting desert plant species to precipitation variability are differentially regulated by soil moisture and nitrogen dynamics. Global Change Biol. 15:1214–1229.

Rogers, A. and S.W. Humphries. 2000. A mechanistic evaluation of photosynthetic acclimation at elevated CO_2. Global Change Biol. 6:1005–1011.

Sacks, W., D.S. Schimel, R.K. Monson and B.H. Braswell. 2006. Model-data synthesis of diurnal and seasonal CO_2 fluxes at Niwot Ridge, Colorado. Global Change Biol. 12:240–259.

Sala, A. and J.D. Tenhunen. 1996. Simulations of canopy net photosynthesis and transpiration in *Quercus ilex* L. under the influence of seasonal drought. Agric. Forest Meteorol. 78:203–222.

Sellers, P.J., D.A. Randall, G.J. Collatz, J.A. Berry, C.B. Field, D.A. Dazlich, C. Zhang, G.D. Collelo and L. Bounoua. 1996. A revised land surface parameterization (SiB2) for atmospheric GCMs. Part I: modeling formulation. J. Climate 9:676–705.

Sharkey, T.D., A.J. Bernacchi, G.D. Farquhar and E.L. Singsaas. 2007. Fitting photosynthetic carbon dioxide response curves for C_3 leaves. Plant, Cell Environ. 30:1035–1040.

Silva, M.E.S., S.H. Franchito and V.B. Rao. 2006. Effects of Amazonian deforestation on climate: a numerical experiment with a coupled biosphere–atmosphere model with soil hydrology. Theoret. Appl. Climatol. 85:1–18.

Su, Y.H., G.F. Zhu, Z.W. Miao, Q. Feng and Z.Q. Chang. 2009. Estimation of parameters of a biochemically based model of photosynthesis using a genetic algorithm. Plant, Cell Environ. 32:1710–1723.

Svensson, M., P.E. Jansson, D. Gustafson, D.B. Kleja, O. Langvall and A. Lindroth. 2008. Bayesian calibration of a model describing carbon, water and heat fluxes for a Swedish boreal forest stand. Ecol. Model. 213:331–344.

Tcherkez G.G.B., G.D. Farquhar and T.J. Andrews. 2006. Despites low catalysis and confused substrate specificity, all ribulose bisphosphate carboxylases may be nearly perfectly optimized. Proc. Natl Acad. Sci. USA 103:7246–7251.

Tuzet, A., A. Perrier and R. Leuning. 2003. A coupled model of stomatal conductance, photosynthesis and transpiration. Plant, Cell Environ. 26:1097–1116.

Tyul, F., R. Gerlach and K. Mengersen. 2008. A comparison of Bayes–Laplace, Jeffreys, and other priors: the case of zero events. Am. Stat. 62:40–44.

Van Oijen, M., J. Rougier and R. Smith. 2005. On Bayesian calibration and evaluation of process-based forest models: bridging the gap between models and data. Tree Physiol. 25:915–927.

Vano, J.A., J.A. Foley, C.J. Kucharik and M.T. Coe. 2006. Evaluating the seasonal and interannual variations in water balance in northern Wisconsin using a land surface model. J. Geophys. Res. 111: G02025, Von Caemmerer, S. 2000. Techniques in plant sciences. Volume 2: biochemical models of leaf photosynthesis. CSIRO Publishing, Collingwood, Victoria, Australia.

Von Caemmerer, S. and G.D. Farquhar. 1981. Some relationships between the biochemistry of photosynthesis and the gas exchange of leaves. Planta 153:376–387.

Von Caemmerer, S., J.R. Evans, G.S. Hudson and T.J. Andrews. 1994. The kinetics of ribulose-1,5-bisphosphate carboxylase/oxygenase in-vivo inferred from measurements of photosynthesis in leaves of transgenic tobacco. Planta 195:88–97.

Walker, G.R., L. Zhang, T.W. Ellis, T.J. Hatton and C. Petheram. 2002. Estimating impacts of changed land use on recharge: review of modeling and other approaches appropriate for management of dry land salinity. Hydrogeol. J. 10:68–90.

Wang, Y.P., R. Leuning, H.A. Cleugh and P.A. Coppin. 2001. Parameter estimation in surface exchange models using nonlinear inversion: how many parameters can we estimate and which measurements are most useful? Global Change Biol. 7:495–510.

Warren, C.R. and E. Dreyer. 2006. Temperature response of photosynthesis and internal conductance to CO_2: results from two independent approaches. J. Exp. Bot. 57:3057–3067.

White, J.D., N.A. Scott, A.I. Hirsch and S.W. Running. 2006. 3-PG productivity modeling of regenerating Amazon forests: climate sensitivity and comparison with MODIS-derived NPP. Earth Interact. 10:1–26.

Williams, M., P.A. Schwarz, B.E. Law, J. Irvine and M.R. Kurpius. 2005. An improved analysis of forest carbon dynamics using data assimilation. Global Change Biol. 11:89–105.

Wilson, K.B., D.D. Baldocchi and P.J. Hanson. 2000. Spatial and seasonal variability of photosynthetic parameters and their relationship to leaf nitrogen in a deciduous forest. Tree Physiol. 20:565–578.

Wohlfahrt, G., M. Bahn, E. Haubner, I. Horak, W. Michaeler, K. Rottmar, U. Tappeiner and A. Cernusca. 1999. Inter-specific variation of the biochemical limitation to photosynthesis and related leaf traits of 30 species from mountain grassland ecosystems under different land use. Plant Cell Environ. 22:1281–1296.

Wullschleger, S.D. 1993. Biochemical limitations to carbon assimilation in C_3 plants – a retrospective analysis of the A/C_i curves from 109 species. J. Exp. Bot. 44:907–920.

Xu, L.K. and D.D. Baldocchi. 2003. Seasonal trends in photosynthetic parameters and stomatal conductance of blue oak (*Quercus douglasii*) under prolonged summer drought and high temperature. Tree Physiol. 23:865–877.

Zhu, G.F., Z.Z. Li, Y.H. Su, J.Z. Ma and Y.Y. Zhang. 2007. Hydrogeochemical and isotope evidence of groundwater evolution and recharge in Minqin Basin, Northwest China. J. Hydrol. 333:239–251.

Zhu, G.F., X. Li, Y.H. Su and C.L. Huang. 2010. Parameterization of a coupled CO_2 and H_2O gas exchange model at the leaf scale of *Populus euphratica*. Hydrol. Earth Syst. Sci. 14:419–431.